

Conf-930572--6

UCRL-JC-112711  
PREPRINT

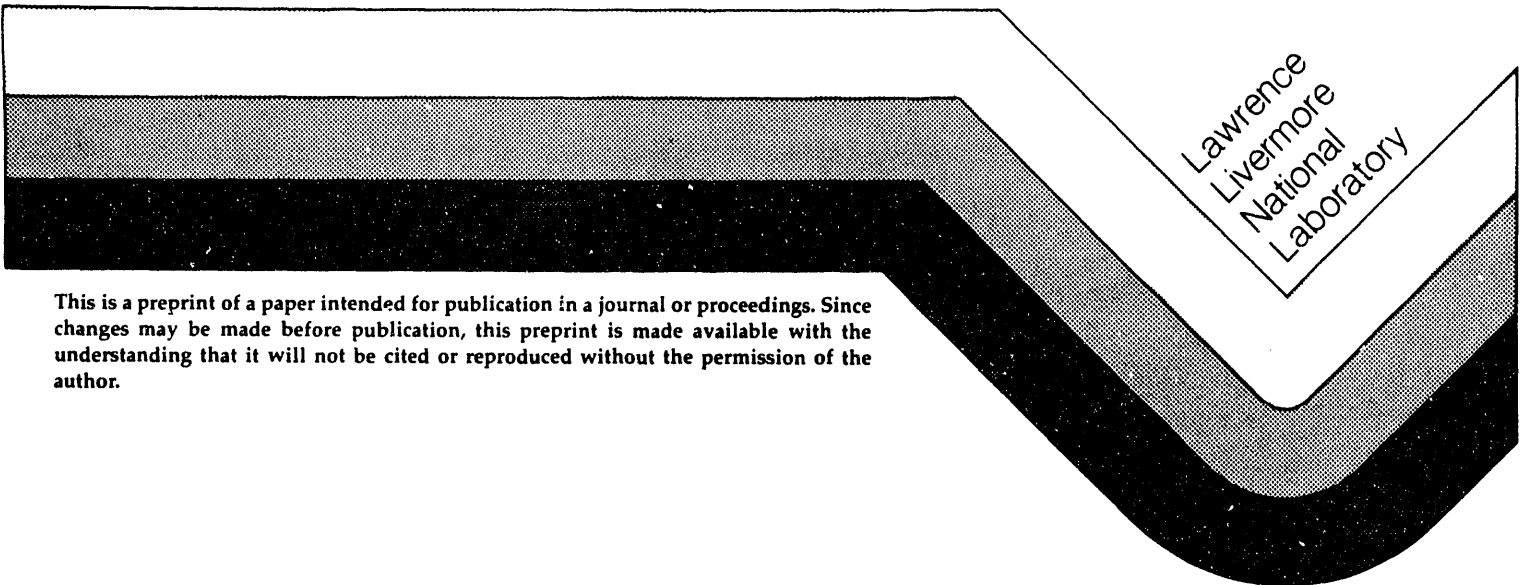
RECEIVED  
JUN 04 1993  
OSTI

**Experimental Studies of Actinide Volatilities  
with Application to Mixed Waste Oxidation Processors**

Oscar H. Krikorian  
Bartley B. Ebbinghaus  
Ralph H. Condit  
Martyn G. Adamson  
Alfred S. Fontes, Jr.  
Dennis L. Fleming

This paper was prepared for presentation at the  
1993 Incineration Conference  
to be held in Knoxville, TN  
May 3-7, 1993

April 30, 1993



This is a preprint of a paper intended for publication in a journal or proceedings. Since changes may be made before publication, this preprint is made available with the understanding that it will not be cited or reproduced without the permission of the author.

#### DISCLAIMER

This document was prepared as an account of work sponsored by an agency of the United States Government. Neither the United States Government nor the University of California nor any of their employees, makes any warranty, express or implied, or assumes any legal liability or responsibility for the accuracy, completeness, or usefulness of any information, apparatus, product, or process disclosed, or represents that its use would not infringe privately owned rights. Reference herein to any specific commercial products, process, or service by trade name, trademark, manufacturer, or otherwise, does not necessarily constitute or imply its endorsement, recommendation, or favoring by the United States Government or the University of California. The views and opinions of authors expressed herein do not necessarily state or reflect those of the United States Government or the University of California, and shall not be used for advertising or product endorsement purposes.

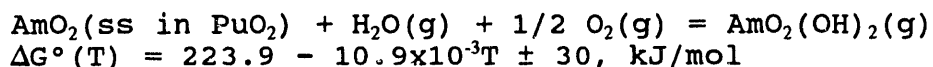
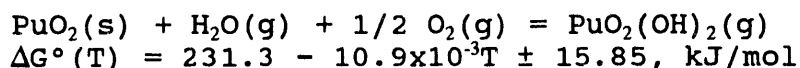
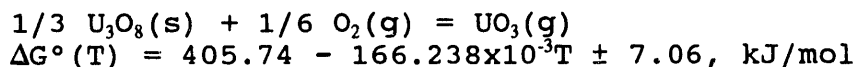
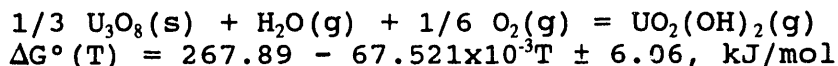
**EXPERIMENTAL STUDIES OF ACTINIDE VOLATILITIES WITH APPLICATION TO MIXED WASTE OXIDATION PROCESSORS\***

Oscar H. Krikorian  
Bartley B. Ebbinghaus  
Ralph H. Condit  
Martyn G. Adamson  
Alfred S. Fontes, Jr.  
Dennis L. Fleming

University of California  
Lawrence Livermore National Laboratory  
P.O. Box 808  
Livermore, CA 94551

**ABSTRACT**

The transpiration technique is used to measure volatilities of U from  $U_3O_8(s)$ , Pu from  $PuO_2(s)$  and Pu and Am from  $PuO_2/2\%AmO_2(s)$  in the presence of steam and oxygen at temperatures ranging from 900 to 1300°C. From the volatility data, the thermodynamics of formation of  $UO_2(OH)_2(g)$ ,  $UO_3(g)$ ,  $PuO_2(OH)_2(g)$ , and  $AmO_2(OH)_2(g)$  are summarized as follows:



These results have been applied to the Rocky Flats Plant Fluidized Bed Incinerator to assess the amount of volatile U, Pu, and Am that would be produced in the secondary combustion chamber. Taking an operating temperature of 550°C, 40 kmols/h of total gas flow at 1 atm pressure, 0.1 atm of  $O_2(g)$ , 0.05 atm of  $H_2O(g)$ , 6000 h of operating time per year, assuming sufficient U and Pu are present in the bed to form  $U_3O_8(s)$  and  $PuO_2(s)$ , and assuming Am is present at 200 ppm in the  $PuO_2(s)$ , gives volatilization rates of  $7.6 \times 10^{-4}$  gU/y,  $7.0 \times 10^{-6}$  gPu/y, and  $4 \times 10^{-9}$  gAm/y in the offgas from the secondary combustion chamber.

\*Work performed under the auspices of the U. S. Department of Energy by the Lawrence Livermore National Laboratory under Contract W-7405-ENG-48.

DISTRIBUTION OF THIS DOCUMENT IS UNLIMITED *EP*

## INTRODUCTION

This work was conducted in support of the Rocky Flats Plant Fluidized Bed Incinerator development. The objective of this study has been to conduct experiments to identify the types and amounts of vapor species of U, Pu, and Am that will be produced in the offgases of mixed waste oxidation processors.

Based on available or predicted thermodynamic data (1-3), a small amount of U, Pu, and Am will be vaporized as  $\text{UO}_2(\text{OH})_2(\text{g})$ ,  $\text{UO}_3(\text{g})$ ,  $\text{PuO}_2(\text{OH})_2(\text{g})$ , and  $\text{AmO}_2(\text{OH})_2(\text{g})$  in mixed waste thermal oxidation processors. Also, if halogen gases such as HCl and HF are present in concentrations greater than about 0.1% in the combustion gas, then actinide oxyhalide vapor species will be important in the offgas and may dominate over the actinide oxyhydroxides (2). The HCl and HF concentrations are expected to be very low in the Rocky Flats Plant Fluidized Bed Incinerator because of the  $\text{Na}_2\text{CO}_3(\text{s})$  present in the bed which reacts with the HCl and HF gasses to produce  $\text{NaCl}(\text{s})$  and  $\text{NaF}(\text{s})$ . The actinide oxyhalide volatilities are therefore expected to be much smaller than the actinide oxyhydroxide volatilities.

## BACKGROUND

The thermodynamics of  $\text{UO}_3(\text{g})$  are well established. Ackermann, et al. (4) and Dharwadkar, et al. (1) have independently carried out transpiration experiments on  $\text{U}_3\text{O}_8(\text{s})$  in the presence of  $\text{O}_2(\text{g})$  which are in good agreement. Dharwadkar, et al. (1) in their work have also carried out transpiration experiments on  $\text{U}_3\text{O}_8(\text{s})$  in the presence of  $\text{O}_2(\text{g})$  and  $\text{H}_2\text{O}(\text{g})$  and identified the species  $\text{UO}_2(\text{OH})_2(\text{g})$ .

No thermodynamic measurements exist for the species  $\text{PuO}_2(\text{OH})_2(\text{g})$  or  $\text{AmO}_2(\text{OH})_2(\text{g})$ . Krikorian (2,3), however, has estimated thermodynamics for these species. The  $\Delta H_f^\circ(298)$  value for  $\text{PuO}_2(\text{OH})_2(\text{g})$  (2) was estimated from bond energy correlations which relate metal fluoride to metal hydroxide bond energies and the  $\Delta H_f^\circ(298)$  value for  $\text{AmO}_2(\text{OH})_2(\text{g})$  (3) was estimated based on trends in actinide oxyhydroxide and oxyhalide bond energies. The entropy and free energy functions were estimated using an empirical relationship which is derived from known thermodynamic values for other oxyhydroxide species.

## APPROACH

The approach used here to obtain U, Pu, and Am volatilities is to apply the transpiration technique to experimentally measure U volatility from  $\text{U}_3\text{O}_8(\text{s})$ , Pu volatility from  $\text{PuO}_2(\text{s})$ , and Pu and Am volatilities from  $\text{PuO}_2/2\%\text{AmO}_2(\text{s})$  in the presence of  $\text{O}_2(\text{g})$  and  $\text{H}_2\text{O}(\text{g})$ . In the transpiration technique, a known amount of carrier gas is passed over a solid or liquid in a furnace chamber such that any volatile gases produced become entrained in the carrier gas and are swept out of the chamber. The volatilized gas then condenses on a substrate that is later removed and quantitatively analyzed for U, Pu, and Am. The carrier gases may also contain reactive gases which enhance the volatility. In this case,  $\text{O}_2(\text{g})$  and  $\text{H}_2\text{O}(\text{g})$  are used. By making measurements on pure  $\text{U}_3\text{O}_8(\text{s})$  and  $\text{PuO}_2(\text{s})$  an upper

limit of U and Pu volatility in thermal oxidizers is established. Interactions of U, Pu, and Am with ash in the thermal processor are expected to lower the  $U_3O_8(s)$ ,  $PuO_2(s)$ , and  $AmO_2(s)$  activities and therefore produce lower volatilities. In working with Am, we were limited in the amount that we could handle in our glove box system. The 2% $AmO_2(s)$  in  $PuO_2(s)$  was chosen to give adequate detectability of the Am. Measurements on all the actinide oxides were made at temperatures high enough to detect U, Pu, and Am volatility, i.e., 900 to 1300°C. Results were then extrapolated to lower temperatures, i.e. 550°C, for the Rocky Flats Plant Fluidized Bed Incinerator.

## **EXPERIMENTAL**

### **Sample Materials**

The sample of  $U_3O_8(s)$  used was obtained from the National Institute of Science and Technology. The purity is given as 99.94% pure  $U_3O_8(s)$ . The sample was characterized by X-ray analysis both before and after the transpiration runs. Before use, a mixture of orthorhombic and hexagonal  $U_3O_8(s)$  was identified with traces of what appeared to be  $UO_3 \cdot 2H_2O(s)$ . After the transpiration runs, the material was identified to be almost pure orthorhombic  $U_3O_8(s)$  with traces of hexagonal  $U_3O_8(s)$ .

The sample of  $PuO_2(s)$  used in the runs had been formed from electrorefined plutonium. It was characterized by mass spectrometric analysis as having an isotopic composition of  $^{238}Pu$  0.014%,  $^{239}Pu$  93.844%,  $^{240}Pu$  5.872%,  $^{241}Pu$  0.221%,  $^{242}Pu$  0.049%, and  $^{241}Am$  0.0264%, all on the basis of metal content. An X-ray diffraction pattern of the  $PuO_2(s)$  starting material showed single phase  $PuO_2(s)$  but with broadened lines consistent with a very fine particulate powder. An X-ray diffraction pattern taken after the transpiration runs also showed single phase  $PuO_2(s)$  but with sharp spotty lines indicating large crystals.

The  $PuO_2/2\%AmO_2(s)$  sample was a reactor grade material. It was characterized by mass spectrometric analysis as having  $^{238}Pu$  0.065%,  $^{239}Pu$  80.659%,  $^{240}Pu$  17.827%,  $^{241}Pu$  0.989%,  $^{242}Pu$  0.460%, and  $^{241}Am$  2.056%, all on the basis of metal content.

### **Experimental Apparatus**

A schematic diagram of the transpiration apparatus for the  $U_3O_8$  transpiration experiments is outlined in Fig. 1. This apparatus is similar in design to that used for the  $PuO_2$  and the  $PuO_2/2\%AmO_2$  experiments. The  $O_2$  and Ar gas flow are regulated by Precision Flow Devices PFD-401 mass flow controllers. These flow meters are accurate to  $\pm 1\%$  and reproducible to  $\pm 0.1\%$  of the full scale reading. The water vapor pressure is regulated by the temperature of the water saturator. Heating tapes kept at around 160°C are used on the inlet and outlet lines to prevent the water vapor from condensing. The mixture of  $O_2/Ar/H_2O$  is passed into the furnace tube and over the actinide oxide sample powders. For the  $U_3O_8$  experiments, an alumina tube, 4.5 cm OD, is used in a platinum wound Marshall furnace which has a uniform temperature hot zone of

13 cm. For the  $\text{PuO}_2$  and  $\text{PuO}_2/2\%\text{AmO}_2$  experiments, a quartz tube, 2.6 cm OD, is used in a Thermcraft clamshell furnace containing Kanthal heating elements. The uniform temperature hot zone is about 7 cm. Quartz or platinum boats are used to hold the  $\text{U}_3\text{O}_8$  powder and alumina boats are used to hold the  $\text{PuO}_2$  and  $\text{PuO}_2/2\%\text{AmO}_2$  powders. The water vapor is collected after passing through the furnace chamber in a Dreirite cartridge (anhydrous  $\text{CaSO}_4(\text{s})$ ) which is weighed both before and after each experiment to determine the total amount of water passed over the sample during each experiment. The  $\text{O}_2$  and Ar gases exiting the system are monitored by a PFD-401 mass flow controller.

In the transpiration experiments on  $\text{U}_3\text{O}_8(\text{s})$ , the uranium vapor species are collected on the inside of a 6mm OD silica glass tube. The exiting gas passes through the collection tube and any volatilized uranium species are collected on it. In the transpiration experiments on  $\text{PuO}_2(\text{s})$  and  $\text{PuO}_2/2\%\text{AmO}_2(\text{s})$ , the actinide vapor species are collected on silica glass wool which is placed downstream of the sample boat. In run #44 of the Pu and Am experiments, a collection tube was used which was similar to that used in the U experiments.

#### **Sample Analyses**

Analyses for uranium were obtained by inductively coupled plasma mass spectrometry. This technique is sensitive enough to detect as little as one nanogram of U. The U on the collection tube is removed by dissolving off the deposit using 8M  $\text{HNO}_3$  solution to which a few drops of concentrated HF have been added. The collection tubes are kept in the solution for a period of at least 24 hr to allow all of the U to dissolve. The sample analyses are estimated to be accurate to within  $\pm 5\%$ .

Pu and Am analyses were obtained by alpha counting. The Pu and Am collection samples were dissolved in the same manner as the U. For the Pu analyses, an aliquot of the resulting solution was then dried on a planchet and counted for alpha activity. In samples from the  $\text{PuO}_2/2\%\text{AmO}_2$  tests, the solutions were passed through an ion exchange column for separation of Pu and Am. Aliquots were then taken down to dryness and alpha counting was used for the Pu and Am determinations.

#### **ANALYSIS OF RESULTS**

The results of the transpiration runs on  $\text{U}_3\text{O}_8(\text{s})$  are given in Table I, and the results of the transpiration runs on  $\text{PuO}_2(\text{s})$  and  $\text{PuO}_2/2\%\text{AmO}_2(\text{s})$  are given in Tables II and III.

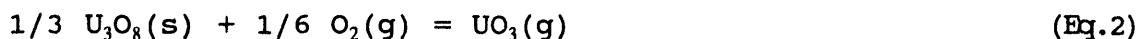
For the  $\text{U}_3\text{O}_8$  experiments, a number of runs were made at  $1100^\circ\text{C}$  with  $p(\text{H}_2\text{O}) = 0.60$  atm where the flow rate was varied. At very slow flow rates in transpiration experiments, erroneously high volatilities are measured due to diffusion. At very high flow rates, erroneously low volatilities are obtained since the gas has insufficient time to equilibrate with the sample. The region of flow rates over which the measured volatility is constant is called

the plateau region. In the  $U_3O_8$  experiments, the plateau region exists from about 10  $cm^3/min$  to at least 250  $cm^3/min$ . Due to greater uncertainties in the data, the same flow rate tests on the  $PuO_2$  and the  $PuO_2/2\%AmO_2$  experiments could not be made. From the  $U_3O_8$  experiments, we expect that similar flow rates give rise to equilibrium values. However, the plateau region may be shifted to lower flow rates since the diameter of the tube used was smaller for the  $PuO_2(s)$  and the  $PuO_2/2\%AmO_2(s)$  volatility studies.

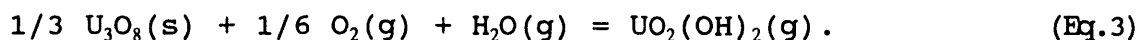
For the  $U_3O_8$  experiments, increased volatility of uranium was observed as the water vapor pressure was increased. This verified the presence of a volatile uranium oxyhydroxide. If the oxyhydroxide vapor species is  $UO_2(OH)_2(g)$ , then at a specified temperature

$$p(U \text{ total})/p(O_2)^{1/6} = A \cdot p(H_2O) + B, \quad (\text{Eq.1})$$

where A and B are constants. Eq.(1) is a result of the combined equilibria from the two volatilization reactions



and



In Fig. 2, a plot of  $p(U \text{ total})/p(O_2)^{1/6}$  versus  $p(H_2O)$  shows an approximately linear relation for a series of experiments run at 1050°C. The two points shown at high water pressures are thought to be uncertain since very low  $O_2$  flow rates were used. Thus, the stoichiometry of the oxyhydroxide is confirmed to be  $UO_2(OH)_2(g)$ .

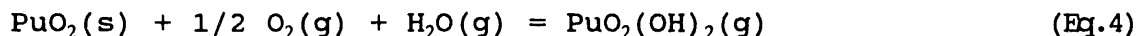
The  $U_3O_8$  volatility results are treated by a 3<sup>rd</sup> law analysis. The free energy function for  $UO_3(g)$  is from Green (5) and the free energy function for  $UO_2(OH)_2(g)$  is calculated from molecular constant data estimates we have made. Table IV gives calculated values of the free energy function for  $UO_2(OH)_2(g)$  at several temperatures. The free energy function of  $U_3O_8(s)$  is from Glusko, et al. (6) and the free energy functions of  $O_2(g)$  and  $H_2O(g)$  are from the JANAF tables (7). To calculate the  $\Delta H_f^\circ(298)$  value for  $UO_2(OH)_2(g)$ , the fraction of  $UO_3(g)$  in the vapor must be accounted for. First, the volatility data with no water present are used to treat Eq.(2) by the 3<sup>rd</sup> law method. This yields  $\Delta H_f^\circ(298)$  as  $423.56 \pm 7.06$  kJ/mol. Using the known  $\Delta H_f^\circ(298)$  value for  $U_3O_8(s)$  from Grenthe, et al. (8) yields  $-768.05 \pm 7.11$  kJ/mol as the  $\Delta H_f^\circ(298)$  value for  $UO_3(g)$ . A similar treatment of the data of Ackermann, et al. (4) yields  $-770.16 \pm 5.58$  kJ/mol as the  $\Delta H_f^\circ(298)$  value for  $UO_3(g)$ , and a similar treatment of the data of Dharwadkar, et al. (1) yields  $-770.80 \pm 1.20$  kJ/mol as the  $\Delta H_f^\circ(298)$  value for  $UO_3(g)$ . Thus, our results agree well with previous experimental work.

Application of the 3<sup>rd</sup> law method to Eq.(3) yields  $278.93 \pm 6.06$  kJ/mol as the  $\Delta H_f^\circ(298)$  value. The  $\Delta H_f^\circ(298)$  value for  $U_3O_8(s)$  given

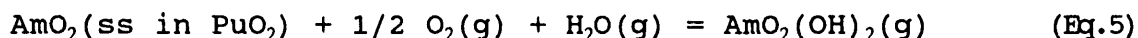
by Grenthe, et al. (8) and the  $\Delta H_f^\circ(298)$  value for  $H_2O(g)$  given in the JANAF tables (7) are then used to calculate  $-1154.51 \pm 6.12$  kJ/mol as the  $\Delta H_f^\circ(298)$  value for  $UO_2(OH)_2(g)$ . A similar treatment of the data of Dharwadkar, et al. (1) yields  $-1211.03 \pm 2.80$  kJ/mol as the  $\Delta H_f^\circ(298)$  value for  $UO_2(OH)_2(g)$ . So far we cannot account for the large discrepancy between the data of Dharwadkar, et al. and this work.

The  $U_3O_8$  volatility data are summarized in Fig. 3 as  $\log K_{eq}$  versus  $10^4/T$  plots for  $UO_3(g)$  and  $UO_2(OH)_2(g)$ . Curves shown are calculated from 3<sup>rd</sup> law analyses of the data.

The  $PuO_2$  and the  $PuO_2/2\%AmO_2$  data are treated using a 3<sup>rd</sup> law analyses. The free energy functions for  $PuO_2(OH)_2(g)$  and  $AmO_2(OH)_2(g)$  are calculated by an equation given by Krikorian (2). The free energy functions for  $PuO_2(s)$  and  $AmO_2(s)$  are taken from Cordfunke, et al. (9) and the free energy functions for  $O_2(g)$  and  $H_2O(g)$  are taken from the JANAF tables (7). Taking the volatilization reactions to be



and



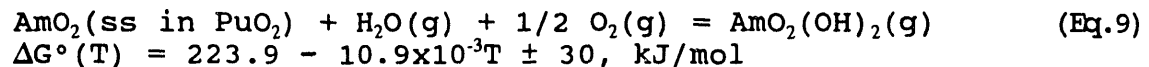
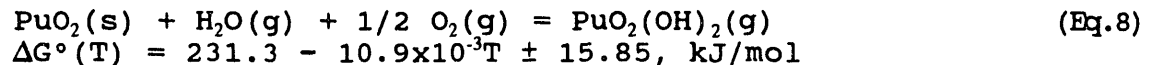
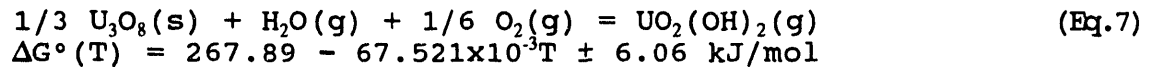
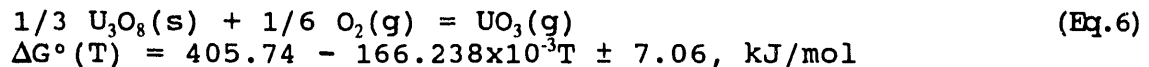
yields  $232.43 \pm 15.85$  kJ/mol as the  $\Delta H_r^\circ(298)$  value for Eq.(4) and  $225 \pm 30$  kJ/mol as the  $\Delta H_r^\circ(298)$  value for Eq.(5) where the activity of  $AmO_2$  is taken as the ideal solution value of 0.021. From the  $\Delta H_f^\circ(298)$  values for  $PuO_2(s)$  and  $AmO_2(s)$  given by Morss (10) and the  $\Delta H_f^\circ(298)$  value for  $H_2O(g)$  given in the JANAF tables (7), the  $\Delta H_f^\circ(298)$  value for  $PuO_2(OH)_2(g)$  is calculated to be  $-1065.60 \pm 15.87$  kJ/mol and the  $\Delta H_f^\circ(298)$  value for  $AmO_2(OH)_2(g)$  is calculated to be  $-949 \pm 30$  kJ/mol.

The calculated equilibrium constants for Eq.(4) and Eq.(5) are summarized in Fig. 4. The data are fit using the curves calculated from the 3<sup>rd</sup> law analyses.

Although we have assumed the gaseous species above  $PuO_2$  and  $PuO_2/2\%AmO_2$  to be  $PuO_2(OH)_2(g)$  and  $AmO_2(OH)_2(g)$ , it is possible, based on the  $U_3O_8(s)$  experiments and other experiments on  $CrO_3(s)$  (11),  $MoO_3(s)$  (12), and  $WO_3(s)$  (13) volatilities in the presence of  $O_2(g)$  and  $H_2O(g)$ , that part of the vapor in the  $PuO_2(s)$  and the  $PuO_2/2\%AmO_2(s)$  experiments is composed of  $PuO_3(g)$  and  $AmO_3(g)$ . However, the equilibrium constant for the generation of  $PuO_3(g)$  or  $AmO_3(g)$  drops off more rapidly with temperature than the equilibrium constant for the generation of  $PuO_2(OH)_2(g)$  or  $AmO_2(OH)_2(g)$ . This tendency is demonstrated by the equilibrium constants for the generation of  $UO_3(g)$  and  $UO_2(OH)_2(g)$  shown in Fig. 3. Thus, the extrapolated values of Pu and Am volatilities at lower temperatures would be lower.



In summary, the thermodynamics of volatilization of  $U_3O_8(s)$ ,  $PuO_2(s)$ , and  $AmO_2(ss \text{ in } PuO_2)$  in the presence of  $O_2(g)$  and  $H_2O(g)$  and temperatures in the range of 800 to 1500 K are summarized as follows:



#### APPLICATION

The Rocky Flats Plant Fluidized Bed Incinerator has two stages. The first stage operates under pyrolyzing conditions and the second operates under excess oxygen. The temperature of each chamber is 550°C. In our analysis, we treat only the second stage. Assuming an offgas composition of  $p(O_2) = 0.10$  atm and  $p(H_2O) = 0.05$  atm and assuming that sufficient U and Pu are present to form  $U_3O_8(s)$  and  $PuO_2(s)$  and that the  $AmO_2(s)$  is present at 200 ppm as solid solution in  $PuO_2(s)$ , the vapor pressures of U, Pu, and Am are calculated to be  $1.3 \times 10^{-15}$  atm,  $1.2 \times 10^{-16}$  atm, and  $7 \times 10^{-20}$  atm, respectively. Assuming 40 kmols/h of gas flow at a pressure of 1 atm and 6000 hours of operating time per year, this amounts to volatilization rates of  $7.6 \times 10^{-5}$  gU/y,  $7.0 \times 10^{-6}$  gPu/y, and  $4 \times 10^{-9}$  gAm/y.

The effect of temperature on the volatility of the actinide oxides in thermal oxidation processes is significant. This is illustrated in Fig. 5 where the volatilization rates of the U, Pu, and Am oxides are given as a function of temperature. The same combustion conditions are assumed as in the Rocky Flats Plant Incinerator except that  $p(H_2O)$  is taken as 0.1 atm rather than 0.05 atm. As a result, a thermal oxidizer operating at 1000°C produces about  $10^5$  times the actinide volatility that would be produced at 550°C. As the offgas cools, the vapor phase actinide species that form under these conditions will be expected to condense on fly ash particulates, as aerosols, and on the system walls.

#### CONCLUSIONS

These transpiration experiments show very low but measurable volatilities of U from  $U_3O_8(s)$ , Pu from  $PuO_2(s)$ , and Pu and Am from  $PuO_2/2\%AmO_2(s)$  from interactions with  $O_2(g)$  and  $H_2O(g)$  and temperatures in the range of 900 to 1200°C. The volatile species are taken to be  $UO_3(g)$ ,  $UO_2(OH)_2(g)$ ,  $PuO_2(OH)_2(g)$ , and  $AmO_2(OH)_2(g)$ . Application of these data to the Rocky Flats Plant Fluidized Bed Incinerator, yields maximum volatilization rates of  $7.6 \times 10^{-5}$  g U/y,  $7.0 \times 10^{-6}$  g Pu/y, and  $4 \times 10^{-9}$  g Am/y.

## REFERENCES

1. S. R. Dharwadkar, S. N. Tripathi, M. D. Karkhanavala, M. S. Chandrasekharaiah, "Thermodynamic Properties of Gaseous Uranium Hydroxide," in Proceedings of the Thermodynamics of Nuclear Materials, vol II, pp. 455-465, 1975.
2. O. H. Krikorian, "Analysis of Plutonium and Uranium Volatilities from mixed wastes in the Molten Salt Processor," in Proceedings of the 1991 Incineration Conference at Knoxville Tennessee, May 15-17, 1991, Univ. of California, EH&S, Irvine, CA 92109, 1991, pp 311-320.
3. O. H. Krikorian, "Predictive Calculations of Volatilities of Metals and Oxides in Steam-Containing Environments," *High Temp.-High Press.*, **14**, 387-397 (1982).
4. R. J. Ackermann, R. J. Thorn, C. Alexander, and M. Tetenbaum, "Free Energies of Formation of Gaseous Uranium, Molybdenum, and Tungsten Trioxides," *J. Phys. Chem.*, **64**, 350-355 (1960).
5. D. W. Green, "Calculation of the Thermodynamic Properties of Fuel Vapor Species from Spectroscopic Data," ANL-CEN-RSD-80-2, 87pp, Argonne National Laboratory, Sept. 1980.
6. V. P. Glusko, L. V. Gurvich, G. A. Bergman, I. V. Veitz, V. A. Medvedev, G. A. Khachkuruzov, V. S. Yungman, Thermodynamic Properties of Individual Substances, Vol IV, High-Temperature Institute, State Institute of Applied Chemistry, National Academy of Sciences U.S.S.R., Moscow (1982).
7. M. W. Chase, C. A. Davies, J. R. Downey, Jr., J. D. Frurip, R. A. McDonald, and A. N. Syverund, **JANAF Thermochemical Tables**, 3<sup>rd</sup> Ed., American Institute of Physics Inc., New York, 1986.
8. I. Grenthe, J. Fuger, R. J. M. Konings, R. J. Lemire, A. B. Muller, C. N.-T. Cregu, H. Wanner, and I. Forest, **Chemical Thermodynamics 1: Chemical Thermodynamics of Uranium**, Nuclear Energy Agency Organization for Economic Co-operation and Development, Elsevier Science Publishing Company, New York (1992).
9. E. H. P. Cordfunke, R. J. M. Konings, P. E. Potter, G. Prins, and M. H. Rand, Thermochemical Data for Reactor Materials and Fission Products, E. H. P. Cordfunke and R. J. M. Konings, eds., North Holland, Amsterdam, 1990.
10. L. R. Morss, "Complex Oxide Systems of the Actinides," in Actinides in Perspective, N. M. Edelstein, ed., Pergamon Press, New York, 1981, pp 381-407.

11. O. Glemser and A. Müller, "The Formation of the Gaseous Hydroxide of Chromium," *Z. anorg. allgen. Chem.*, **334**, 151-154 (1964).
12. G. R. Belton and A. S. Jordan, "The Volatilization of Molybdenum in the Presence of Water Vapor," *J. Phys. Chem.*, **69**(6), 2065-2071 (1965).
13. G. R. Belton and R. L. McCarron, "The Volatilization of Tungsten in the Presence of Water Vapor," *J. Phys. Chem.*, **68**(7), 1852-1856 (1964).

Table I. Summary of run temperatures, flow rates of O<sub>2</sub>(g) plus Ar(g), total moles of O<sub>2</sub>(g), H<sub>2</sub>O(g), and Ar(g) passed, pressures of O<sub>2</sub>(g) and H<sub>2</sub>O(g), collected amount of U, and derived pressures of the U vapor species.

run #	T, K	flow cm <sup>3</sup> /min	total moles	p(O <sub>2</sub> ) atm	p(H <sub>2</sub> O) atm	μg U	p(U) atm
7	1323	50	0.8429	0.4396	0.5604	19.3	9.619x10 <sup>-8</sup>
8	1323	25	0.4112	0.4506	0.5494	9.63	9.839x10 <sup>-8</sup>
9	1323	15	0.3471	0.3204	0.6796	9.52	1.152x10 <sup>-7</sup>
10	1323	56	0.4113	0.4505		7.23	7.385x10 <sup>-8</sup>
11	1323	6	0.3892	0.1143	0.8857	12.4	1.340x10 <sup>-7</sup>
12	1323	25	0.4076	0.4546		3.03	3.123x10 <sup>-8</sup>
14	1323	50	0.8653	0.2146	0.5708	13.96	6.792x10 <sup>-8</sup>
15	1223	56	2.7419	0.5495		1.54	2.360x10 <sup>-9</sup>
17	1473	50	0.5895	0.4190	0.5810	250.9	1.788x10 <sup>-6</sup>
18	1323	9	0.1827	0.2436	0.7564	6.86	1.576x10 <sup>-7</sup>
19	1323	55	0.4076	0.4546		2.97	3.061x10 <sup>-8</sup>
20	1373	100	1.1440	0.4318	0.5682	72.4	2.659x10 <sup>-7</sup>
21	1223	30	3.2453	0.5572	0.4428	5.9	7.638x10 <sup>-9</sup>
22	1373	10	0.1621	0.4571	0.5429	10.4	2.695x10 <sup>-7</sup>
25	1373	300	3.6891	0.4018	0.5982	183	2.084x10 <sup>-7</sup>
26	1323	50	0.6214	0.5962	0.4038	9.03	6.105x10 <sup>-8</sup>
27	1323	50	0.4543	0.8155	0.1845	5.2	4.809x10 <sup>-8</sup>
31	1573	120	0.7377	0.4018	0.5982	1980	1.128x10 <sup>-5</sup>
32	1573	120	2.0938	0.1416	0.8584	3150	6.321x10 <sup>-6</sup>
33	1573	50	0.6819	0.5433	0.4567	2080	1.282x10 <sup>-5</sup>
34	1573	50	0.3705	1.0000		2480	2.812x10 <sup>-5</sup>
46	1373	50	1.1116	1.0000		13.93	5.265x10 <sup>-8</sup>
47	1373	200	2.4746	0.3993	0.6007	162.7	2.762x10 <sup>-7</sup>
49	1473	30	0.2964	1.0000		180	2.551x10 <sup>-6</sup>
50	1273	30	0.5929	1.0000		3.02	2.140x10 <sup>-8</sup>
55	1173	25.0	2.0071	0.3969	0.6035	2.38	1.975x10 <sup>-9</sup>
56	1373	6.0	0.1186	0.4119	0.5881	30.3	4.422x10 <sup>-7</sup>
58	1373	20.0	0.3623	0.3995	0.6005	67.4	3.123x10 <sup>-7</sup>
59	1173	25.0	0.5558	1.0000		1.31	9.902x10 <sup>-9</sup>
60	1373	50.0	1.0499	0.4120	0.5880	148	2.440x10 <sup>-7</sup>

Table II. Summary of run temperatures, flow rates of O<sub>2</sub>(g) plus Ar(g), total moles of O<sub>2</sub>(g), H<sub>2</sub>O(g), and Ar(g) passed, pressures of O<sub>2</sub>(g) and H<sub>2</sub>O(g), collected amounts of Pu, and derived pressures of the Pu vapor species.

run #	T, K	flow cm <sup>3</sup> /min	total moles	p(O <sub>2</sub> ) atm	p(H <sub>2</sub> O) atm	μg Pu	p(Pu) atm
4	1314	500	2.981	0.416	0.169	0.22	3.09x10 <sup>-10</sup>
6	1414	500	1.352	0.459	0.0828	0.975	3.02x10 <sup>-9</sup>
8	1413	500	1.365	0.454	0.0916	1.3	3.98x10 <sup>-9</sup>
9	1316	500	2.728	0.909	0.0913	0.26	3.99x10 <sup>-10</sup>
23	1218	500	5.640	0.916	0.0844	0.178	1.32x10 <sup>-10</sup>
24	1331	500	2.815	0.917	0.0828	0.247	3.67x10 <sup>-10</sup>
25	1433	500	1.462	0.919	0.0814	0.089	2.55x10 <sup>-10</sup>
33	1434	50	0.711	0.523	0.477	0.214	1.26x10 <sup>-9</sup>
34	1334	50	1.390	0.446	0.554	0.081	2.44x10 <sup>-10</sup>
44	1431	50	2.481	0.499	0.501	0.44	7.42x10 <sup>-10</sup>

Table III. Summary of run temperatures, flow rates of O<sub>2</sub>(g) plus Ar(g), total moles of O<sub>2</sub>(g), H<sub>2</sub>O(g), and Ar(g) passed, pressures of O<sub>2</sub>(g) and H<sub>2</sub>O(g), collected amounts of Pu, and derived pressures of the Am vapor species.

run #	T, K	flow cm <sup>3</sup> /min	total moles	p(O <sub>2</sub> ) atm	p(H <sub>2</sub> O) atm	μg Am	p(Am) atm
23	1218	500	5.690	0.916	0.0844	0.016	1.2x10 <sup>-11</sup>
24	1331	500	2.815	0.917	0.0828	0.003	4.4x10 <sup>-12</sup>
25	1433	500	1.462	0.919	0.0814	0.003	8.5x10 <sup>-12</sup>
33	1434	50	0.711	0.523	0.477	0.004	2.3x10 <sup>-11</sup>
34	1334	50	1.390	0.446	0.554	0.001	3.0x10 <sup>-12</sup>
44	1431	50	2.481	0.499	0.501	0.0088	1.5x10 <sup>-11</sup>

Table IV. Calculated free energy function for  $\text{UO}_2(\text{OH})_2(\text{g})$  derived from estimated molecular constants.

T (K)	$-(G^\circ(T) - H^\circ(298)) / T$ ( $\text{Jmol}^{-1}\text{K}^{-1}$ )
800	442.305
900	451.929
1000	461.113
1100	469.855
1200	478.173
1300	486.095
1400	493.649
1500	500.861

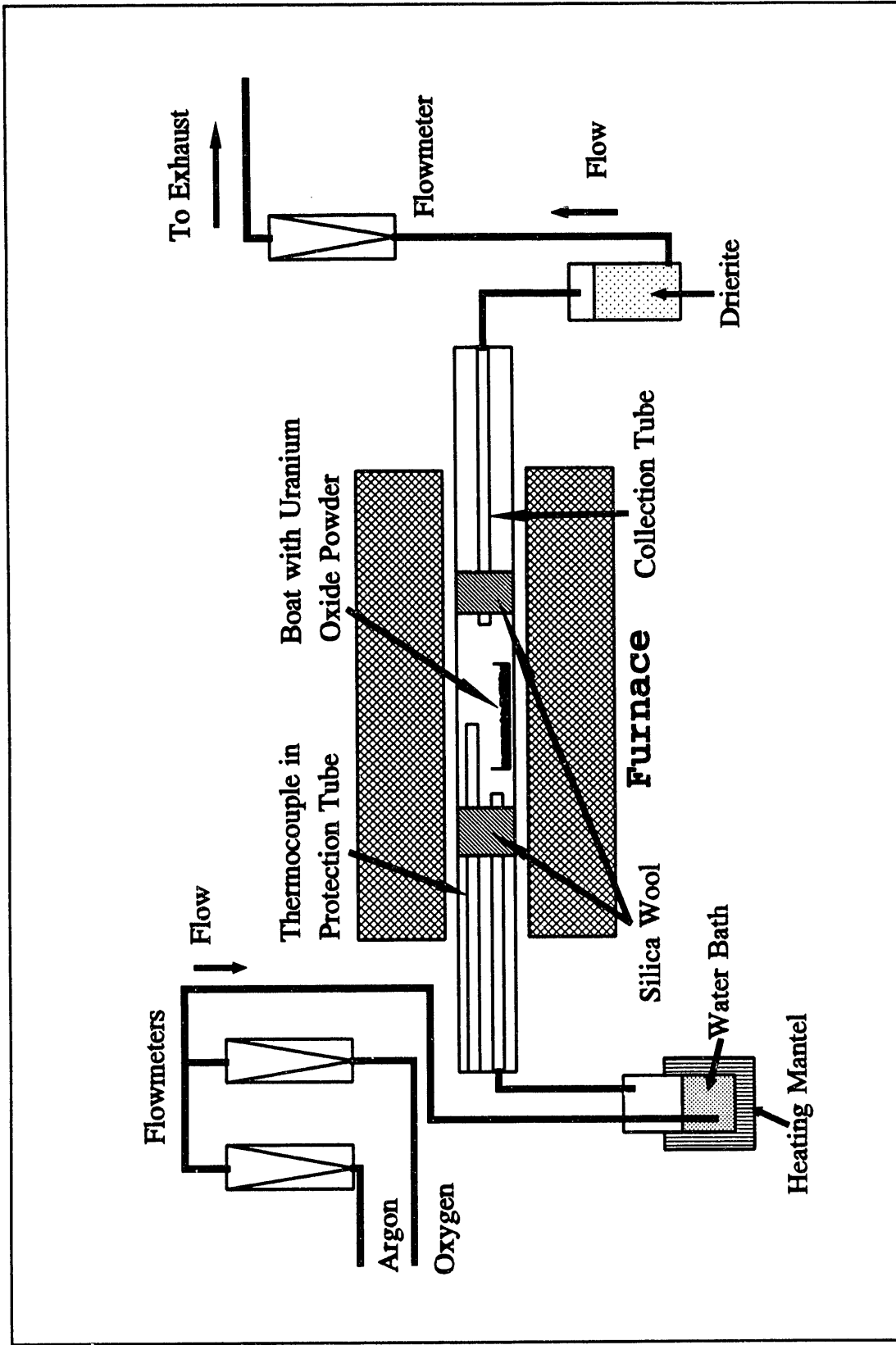


Fig. 1. Schematic diagram of transpiration equipment used in  $U_3O_8(s)$  volatility experiments.



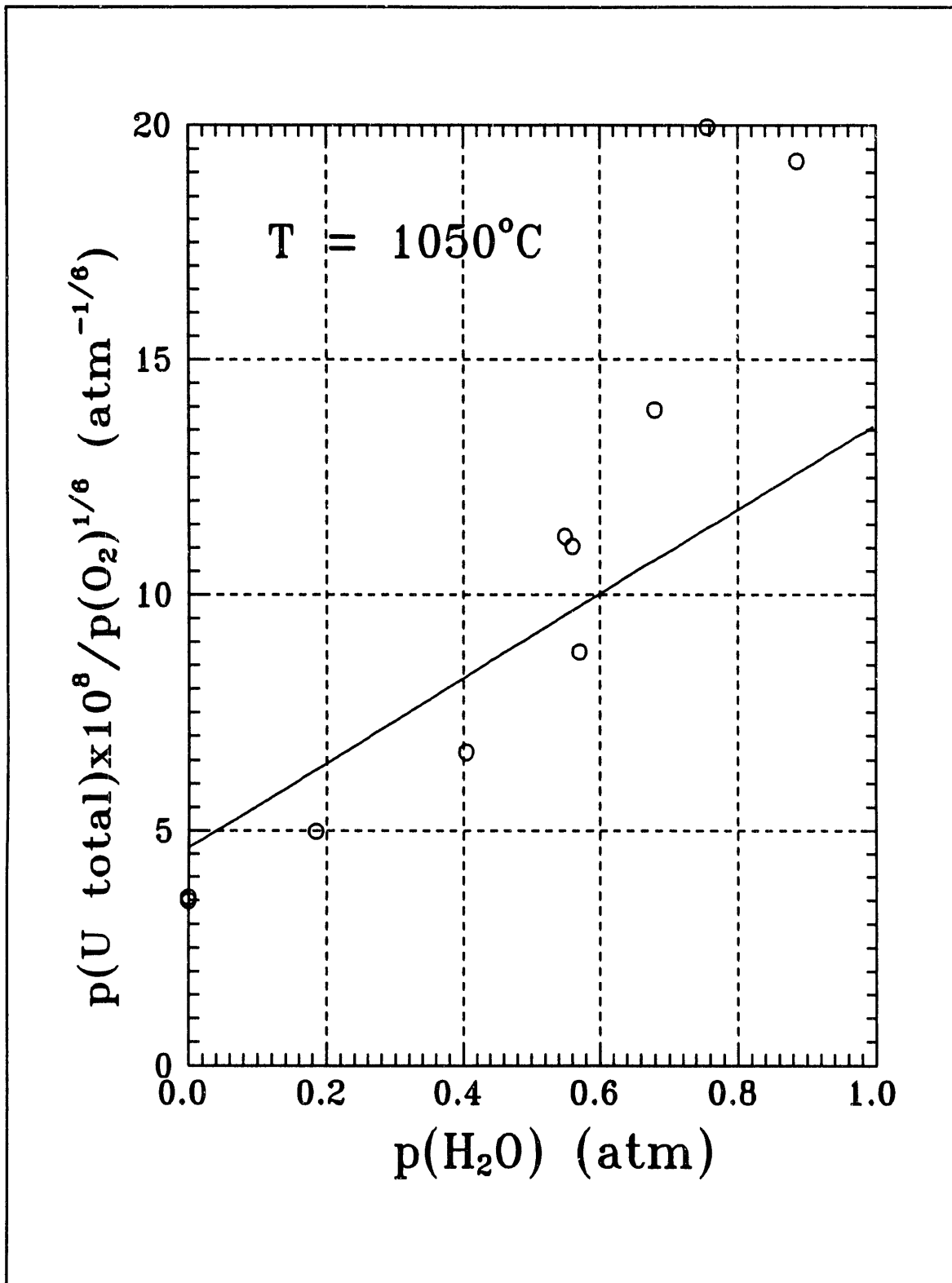


Fig. 2. Plot showing the effect of water vapor pressure on the volatility of  $\text{U}_3\text{O}_8(\text{s})$  at  $1050^{\circ}\text{C}$ .

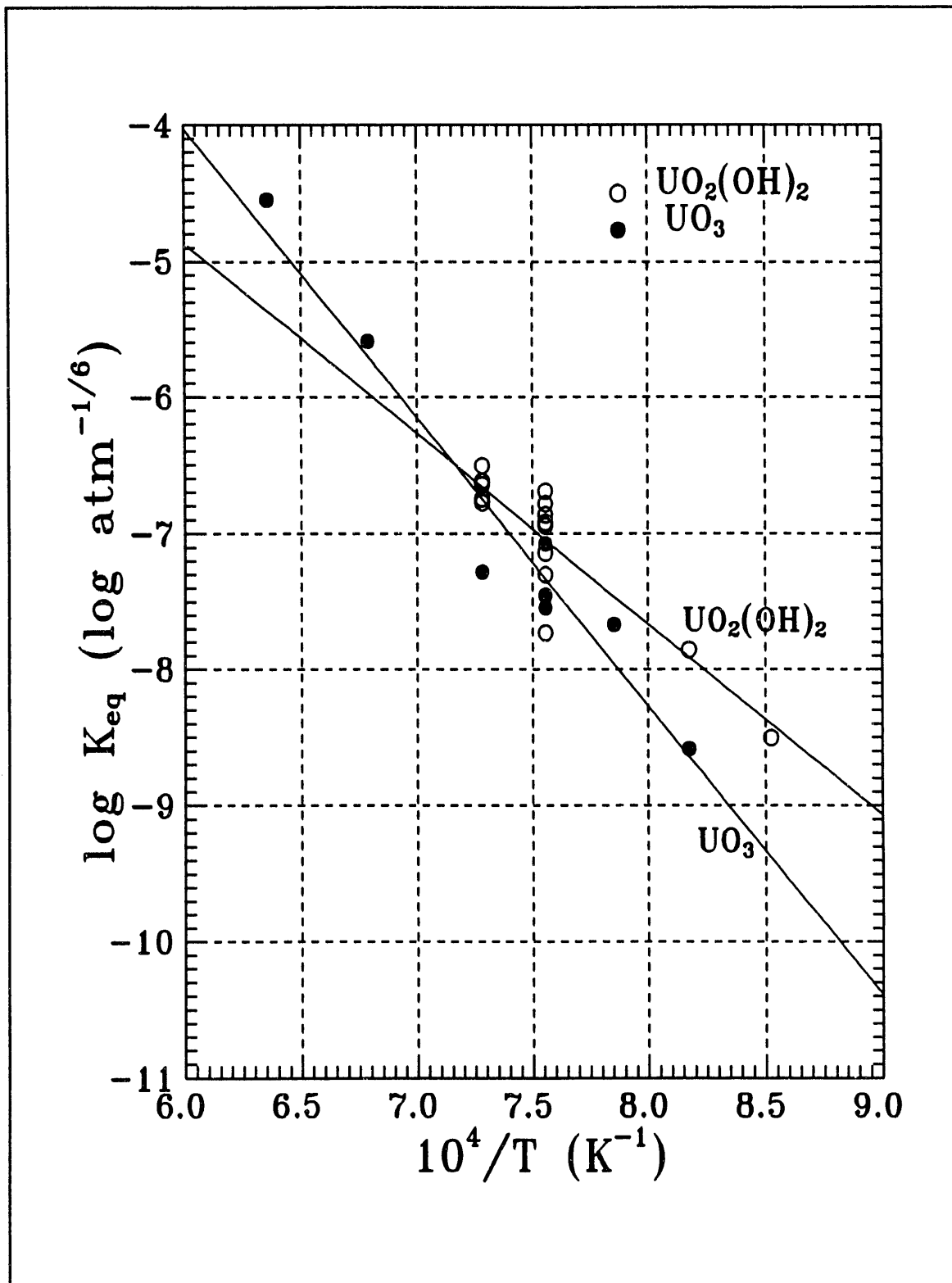


Fig. 3. Plot of  $\log K_{eq}$  versus  $10^4/T$  for Eq.(2) and Eq.(3). Curves were generated from 3<sup>rd</sup> law analyses of the data.

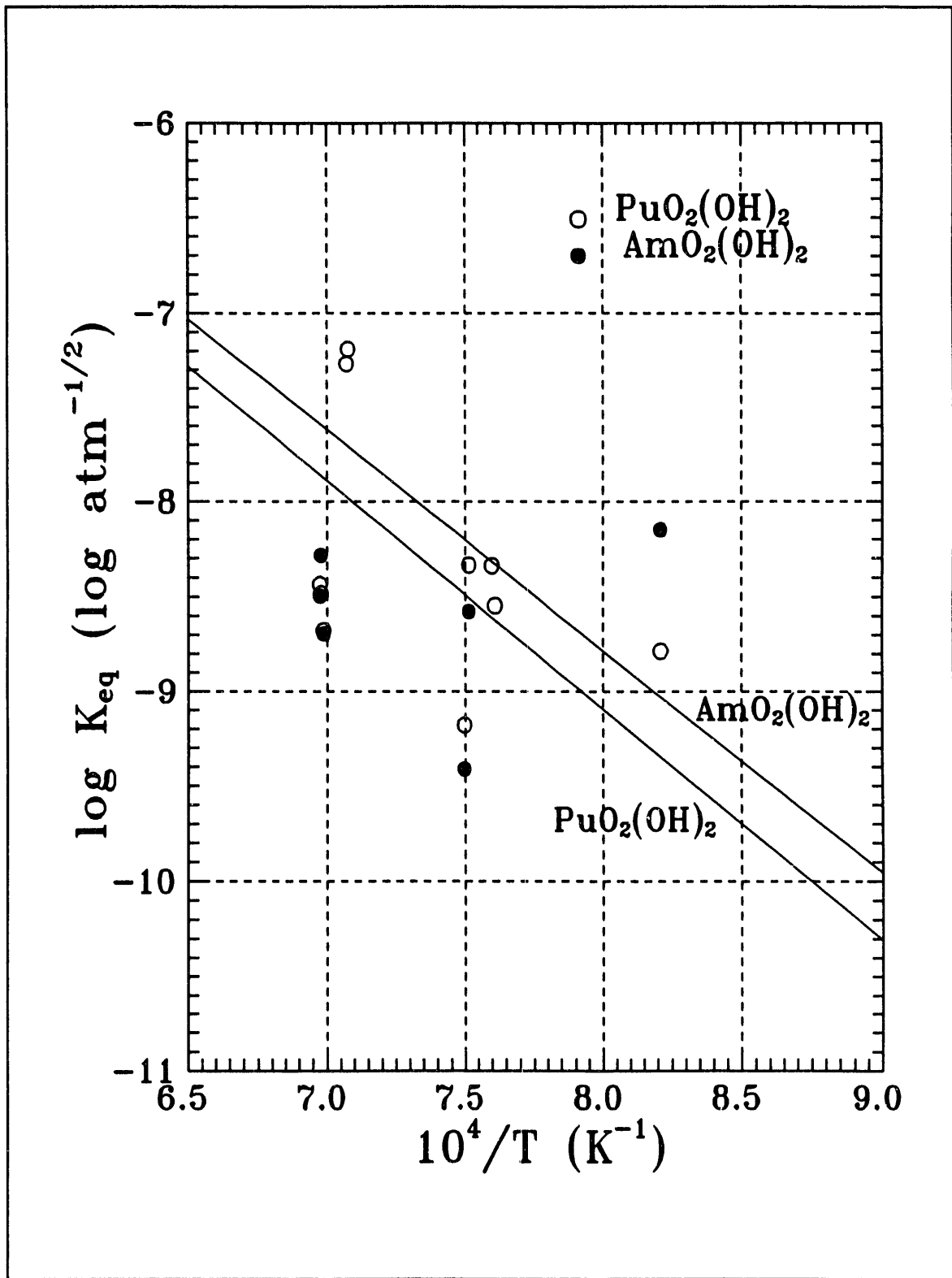


Fig. 4. Plot of  $\log K_{eq}$  versus  $10^4/T$  for Eq.(4) and Eq.(5). Curves were generated from 3<sup>rd</sup> law analyses of the data.

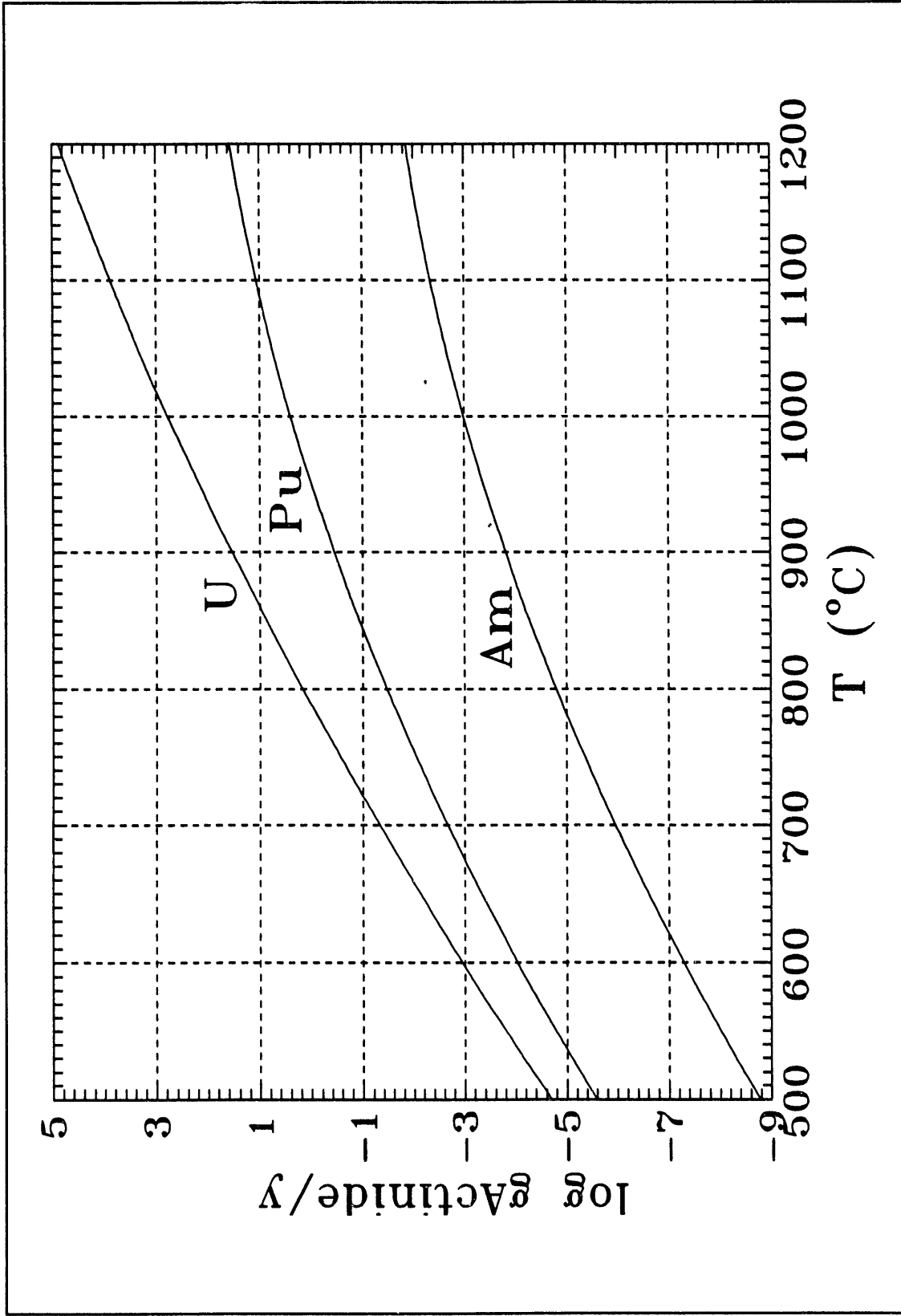


Fig. 5. U, Pu, and Am volatilization rates in log grams per year versus temperature in a mixed waste incinerator.

**END**

---

**DATE  
FILMED**

8 / 10 / 193

